Research Report for the Marshall Plan Foundation

Determining a mechanism of formation for metal-organic frameworks by X-ray crystallography

Cody C. Webb Jr., Syracuse University

1. Introduction

This research report summarizes the work completed on the project that studied the mechanism of formation for a prototypical metal-organic framework (MOF), using a technique called small-angle X-ray scattering (SAXS). MOFs are a diverse class of compounds in inorganic chemistry, and exhibit highly-ordered, porous multi-dimensional crystalline structures [1]. Furthermore, MOF research is of significant interest throughout various fields of chemistry due to the various technically relevant applications of these materials [2].

Despite significant advances since the start of the century, the challenge of synthesizing a target MOF has remained a non-trivial impediment to scientists. There have actually been cases where a new MOF was discovered by incident rather than by design [3]. Traditionally, to gain a comprehensive understanding of a MOF system has required implementing a "trial and error" method, where exhaustive sets of reactions are performed to identify a viable phase [4]. Developing a system for the rational design of new MOFs would greatly simplify this process, and this was the motivation for this work. Our approach submits that determining a mechanism of formation for MOFs would bring a solution to this challenge.

We have elected to study the MOF HKUST-1 (Hong Kong University of Science and Technology), one of the most extensively researched MOFs reported in the literature [5]. HKUST-1 is a copper-based MOF which utilizes the 1,3,5-benzenetricarboxylic acid (H_3BTC, H_3TMA, trimesic acid) ligand. HKUST-1 has been shown to be useful for applications such as the removal of toxic chemical warfare agents [6], the storage of greenhouse gases like methane

[7], and the storage of dihydrogen gas, making HKUST-1 useful to be integrated into hydrogen fuel cells [8]. Furthermore, there have been two recently reported facile synthetic procedures which produce HKUST-1 in-situ, using readily available and inexpensive reagents [9, 10].

Our approach was to apply these synthetic methods with a structural characterization technique called small-angle X-ray scattering (SAXS), in a time-resolved manner. Traditional X-ray diffraction (XRD) techniques provide static structural information on crystalline materials. The advantage for using SAXS is that in addition to collecting crystal structure information similar to XRD, structural information is also provided for amorphous and nanoscale solids. SAXS has been successfully used previously to study MOF formation, including one study involving HKUST-1 where a Keggin-type polyacid was used as a template [11]. This project has aimed to determine the role of the solvent and of the anion of the copper salt in the mechanism of formation of HKUST-1.

This project was a continuation of a collaborative project between my home institution of Syracuse University (Syracuse, NY, USA), and the Graz University of Technology (TU Graz, Graz, Austria). This project was originally conceived in 2013 by my advisor Dr. Karin Ruhlandt, who is now the Dean of the College of Arts & Sciences at Syracuse University, and Dr. Heinz Amenitsch, a professor at TU Graz and the managing beamline scientist at the Austo-SAXS beamline at the Elettra Synchrotron in Trieste, Italy.

My involvement began with the first experiments being conducted at Elettra in January of 2014 with Dr. Ruhlandt, who at the time was a visiting professor of chemistry and a Fulbright Fellow at TU Graz. I continued these experiments with Dr. Amenitsch the following summer during a ten-week stay at TU Graz as an international undergraduate researcher. During these experiments we used a “batch reactor” set-up, where we combined a solution of a copper

precursor with a stirring solution of the ligand (H_3TMA), and we continuously cycled the reaction mixture into the path of the X-ray beam, thereby continuously collecting structural information on the reagents and products. In some cases however, the product formed instantaneously. Additionally, the batch reactor did not provide a homogeneous environment, meaning the reaction could have progressed further in some parts of the reaction vessel than others.

We discovered that because of these issues, this approach would not be able to adequately characterize a MOF mechanism for HKUST-1. The solution I offered in my proposal to the Marshall Plan Foundation, in collaboration with both Dr. Amenitsch and Dr. Ruhlandt, was to utilize a stop-flow set-up. A stop-flow system exerts homogeneous control over the combination of the reagents and can also provide for extremely fast time-resolutions. This report details the experiments we have run to synthesize HKUST-1 using a stop-flow set-up combined with time-resolved SAXS. The series of experiments which we have conducted have resolved the time-resolution challenge, which we were unable to overcome in our preliminary experiments. Finally, our work had adopted a successful synthetic strategy where a series of experiments were performed with systematic manipulation of the solvent system and copper precursor.

2. Methods and Materials

2.1 Reagents and Solution Preparation

All copper reagents were used as received. Copper (II) acetate monohydrate [$Cu(CH_3CO_2)_2 \cdot H_2O$, $Cu(OAc)_2 \cdot H_2O$; ≥98%], copper (II) nitrate hemi(pentahydrate) [$Cu(NO_3)_2 \cdot 2.5H_2O$; 99.99%], copper (II) sulfate ($CuSO_4$, ≥99.0%), and copper (II) chloride dihydrate [$CuCl_2 \cdot 2H_2O$, ≥99.0%] were all acquired from Sigma Aldrich. The ligand 1,3,5-benzenetricarboxylic acid (H_3BTC, H_3TMA, trimesic acid) was also acquired from Aldrich

(95%) and used as received. Solvents used for copper salt and ligand solutions were deionized water, methanol (J. T. Baker, ≥99.8%), ethanol (Fluka Analytical, ≥99.8%), and isopropanol (J. T. Baker, ≥99.7%). All solvents were used without further purification.

Solutions of the ligand and copper salts were prepared according to established literature procedures [9, 10]. The template for preparing these solutions was to use 3.67 mmols of a copper salt combined with 40 mL of a solvent to provide a 0.0918 M solution. $Cu(OAc)_2 \cdot H_2O$ is not soluble in alcohols, so only an aqueous solution was prepared by combining 0.74 g of $Cu(OAc)_2 \cdot H_2O$ with 40 mL of deionized water. Rigorous stirring after several minutes resulted in a light-blue solution. $Cu(NO_3)_2 \cdot 2.5H_2O$ was soluble in all of the solvents, so for four separate solutions approximately 0.84 g of $Cu(NO_3)_2 \cdot 2.5H_2O$ was combined with 40 mL of solvent, respectively. The copper salt dissolved readily with stirring, resulting in solutions which were increasingly blue in color as the solvent polarity decreased. $CuCl_2 \cdot 2H_2O$ was also soluble in each of the solvents. Four solutions were each prepared using 0.62 g of $CuCl_2 \cdot 2H_2O$ combined with 40 mL of water, methanol, ethanol, and isopropanol (respectively). Similarly to the $Cu(NO_3)_2 \cdot 2.5H_2O$ solutions, the solutions of $CuCl_2 \cdot 2H_2O$ exhibited a more intense color (green) as the solvent decreased in polarity. Only an aqueous solution of $CuSO_4$ was prepared as $CuSO_4$ is insoluble in alcohols. The solution was prepared using 0.57 g of $CuSO_4$ and 40 mL of deionized water, resulting in a clear faintly blue solution. Solutions of H_3TMA were prepared using approximately 0.50 g of the ligand and 150 mL of each solvent. After sonication for approximately 10 minutes the solid ligand dissolved resulting in clear solutions. The preparation of the aqueous ligand solution required an addition of 0.6 g (7.14 mmols) of sodium bicarbonate in order to increase the reactivity and solubility of the ligand.

2.2 Equipment Description and Experimental Apparatus

Small-angle X-ray scattering (SAXS) measurements were collected at the Austro-SAXS beamline at the Elettra Synchrotron facility in Basovizza, Italy. The intense synchrotron X-ray radiation was delivered to the beamline from the storage ring at an energy of 8 keV. The beam was passed through a monochrometer to provide X-ray light of wavelength 0.154 nm. The X-ray beam was then collimated and then inserted into the experimental hutch, where the samples were irradiated. The intensity and scattering vector (q, $0.1 \leq q \leq 7$) of the scattered X-rays were then measured by a Dectris 2D Pilatus 1M detector.

When the X-ray beam is opened into the experimental hutch, it is impossible to directly handle any equipment as exposure to these X-rays can be fatal, so a high degree of external control of the equipment was required. Our experimental set-up used a BioLogic (Paris, France) SFM-400 stop-flow instrument. Figure 1 provides an image of the experimental set-up. The instrument itself is seen in Figure 1 as the large black box. The silver stage that the stop-flow instrument sits on top of is a system of motors, which allowed us to change the position of the machine in order to align the sample with the beam, after the beam was turned on. The four beige circular ports on top of the instrument are the places where the reagents were loaded into the instrument.

The silver block in the center of the reagent ports is called the cuvet, and this was the location of the capillary, seen in Figure 1B. The syringe connected to the top of the capillary was filled with approximately 5 mL of deionized water, which acted to stop the flow of the reagents out of the capillary. Importantly, all air bubbles were removed from this syringe as significant amounts of air can cause an imbalanced pressure resulting in a poor injection of the reagents into

the capillary. Inside the base of the cuvet, is the micromixer, where the reagents were combined and vigorously stirred. After a designated amount of stirring time, the product was injected into the capillary where the sample was irradiated by the X-ray beam.

A B

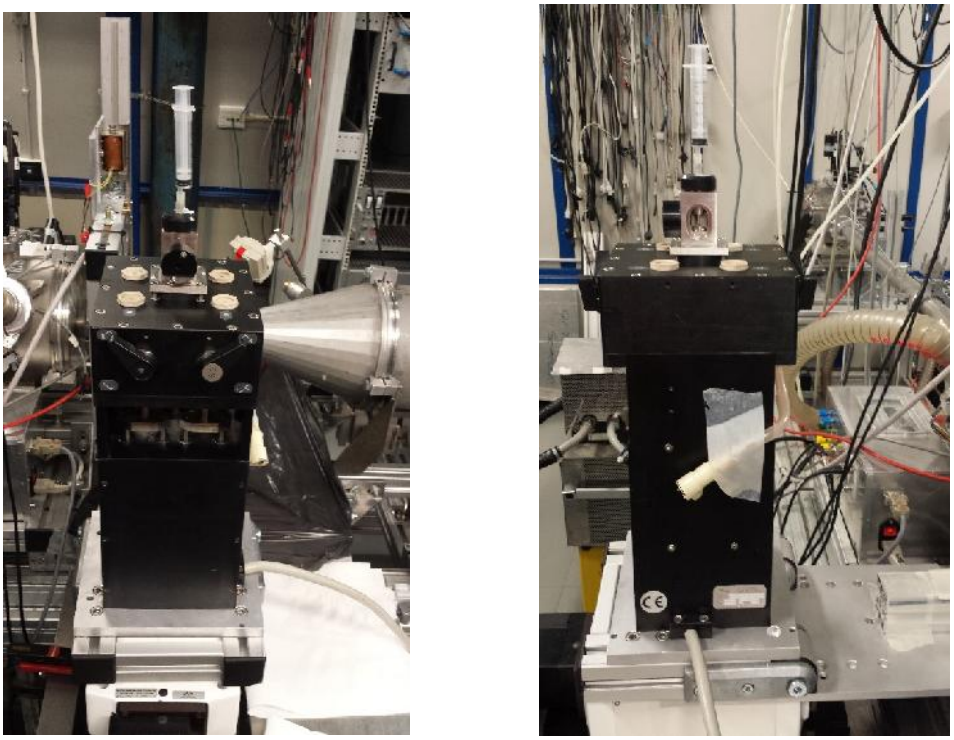

Figure 1. (A)Image of the stop-flow instrument used for our experiments. (B) Side view of the stop-flow instrument where the capillary is now visible.

The volume of reagents injected and the time of mixing the reagents is controlled by a program called the MPS (Motor Power Supply). The stop-flow instrument is connected to a computer which links to an outside computer terminal, where we could set the amount of reagents to inject from any port and for how long these reagents should mix. Initially, approximately 10 mL of the reagent solutions and the solvents were loaded into the stop-flow instrument using syringes. The computer linking to the instrument had a set of controls which allowed us to select a port and then load the reservoirs inside the instrument with the solutions. Great care was taken during this step to ensure that any air bubbles present were removed from

the instrument. Continuous loading and unloading of the reagents from the reservoirs removed all air bubbles from the instrument.

3. Synthetic Strategy

The synthesis of the metal-organic framework (MOF) HKUST-1 was done according to two similar procedures reported in the literature [9, 10]. The four different reactions performed in these experiments are listed in Scheme 1.

$$\text{(A) } 3\ Cu(NO_3)_2 \cdot 2.5H_2O + 2\ H_3TMA \rightarrow [Cu_3(tma)_2]_\infty + 6\ HNO_3 + 7.5\ H_2O$$

$$\text{(B) } 3\ Cu(OAc)_2 \cdot H_2O + 2\ H_3TMA \rightarrow [Cu_3(tma)_2]_\infty + 6\ H(OAc) + 3\ H_2O$$

$$\text{(C) } 3\ CuCl_2 \cdot 2H_2O + 2\ H_3TMA \rightarrow [Cu_3(tma)_2]_\infty + 6\ HCl + 6\ H_2O$$

$$\text{(D) } 3\ CuSO_4 + 2\ H_3TMA \rightarrow [Cu_3(tma)_2]_\infty + 3\ H_2SO_4$$

Scheme 1. The reaction to form HKUST-1 $\{[Cu_3(tma)_2]_\infty\}$ using the copper salt: (A) $Cu(NO_3)_2 \cdot 2.5H_2O$, (B) $Cu(OAc)_2 \cdot H_2O$, (C) $CuCl_2 \cdot 2H_2O$, and (D) $CuSO_4$. Note that this stoichiometry uses reduced coefficients and does not include any solvent molecules which may be coordinated to copper atoms or occupying the cavities of HKUST-1.

The reagents were actually combined in a 6:4 (copper salt to ligand) molar ratio, which is actually twice what is indicated in Scheme 1. The copper salt solution was loaded into port 4 of the stop-flow instrument and the ligand solution was loaded into port 3. Ports 1 and 2 contained the solvents of the copper salt solution and the ligand solution, respectively. The solvents were "pushed" through the instrument at the conclusion of each experiment using the controls on the computer in order to clean the instrument and micromixer. The knobs on the upper-front face of the instrument in Figure 1 were set for each port to control whether the reagents inside the reservoir were pushed through the instrument or were refilling the reservoir. If the knobs were set "down", the reagents were pushed through the instrument, and if the knobs were set "up", then the reagents could be loaded into the instrument. Usually three rounds of cleaning with the pre-loaded solvents were performed prior to a new experiment being conducted.

Once the reagents were properly loaded into the instrument, the knobs for ports 3 and 4 were set into the lower “push” positions. This was not done for ports 1 and 2 because this would have caused a change in the internal pressure of the instrument, thus affecting how the reagents would have been combined. The stop-flow instrument was then lowered, as seen in Figure 2, so that the capillary was aligned with the path of the X-ray beam.

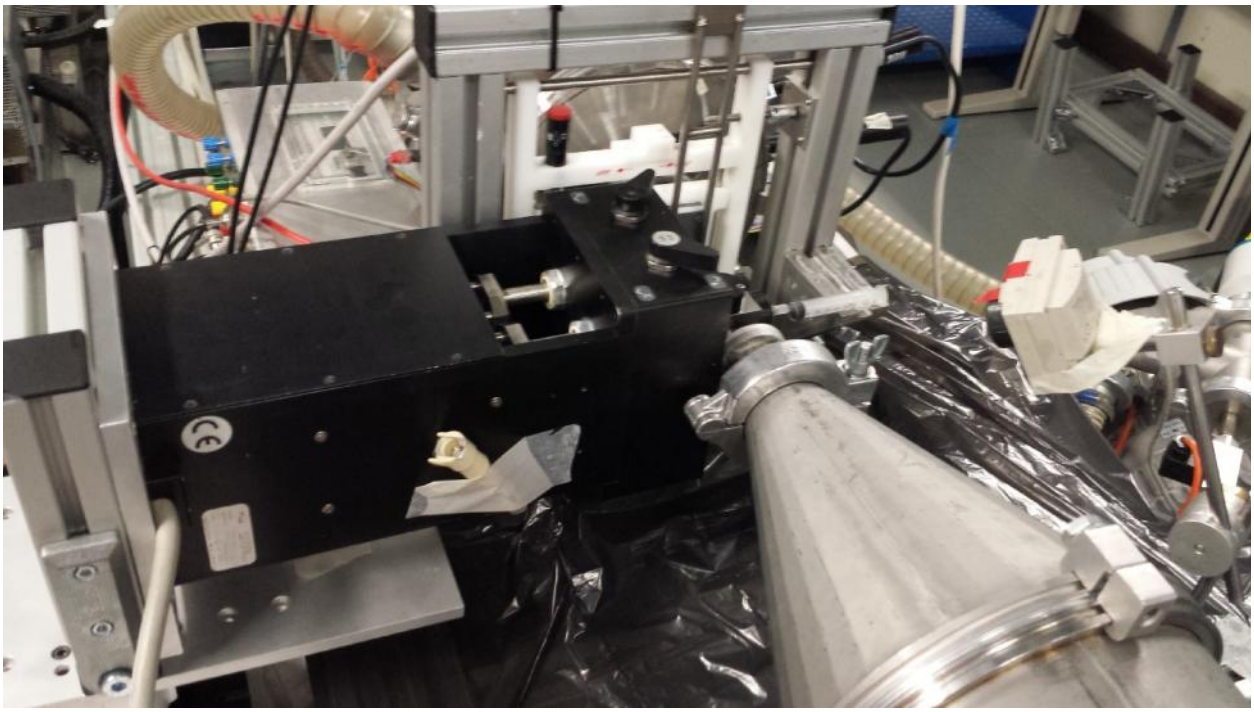

Figure 2. Lowered position of the stop-flow instrument. The black plastic covering below the apparatus was placed in case of any leakage of reagents.

Once the experimental hutch was sealed and the X-ray beam opened through the shutter, a detection system could determine if the capillary was properly aligned with the beam. If it was not, the motors on the stop-flow instrument were adjusted accordingly. Once the capillary was aligned, along with optimization of the monochrometer and the photodiode, the experiments could then be set up on the MPS. The experiment for collecting data on the background was set up in three steps:

Step 1: 200 μL (microliters) of the solvent for the copper salt solution were injected for 100 ms (milliseconds).
Step 2: 200 μL of the solvent for the ligand solution were injected for 100 ms.
Step 3: 240 μL of the copper salt solution solvent + 160 μL of the ligand solution were simultaneously injected for 100 ms.

In the first two steps of this process, the solvents act to flush out any solid which may have been left in the capillary. The final step injects the solvents in the same 6:4 ratio as their corresponding copper salt and ligand solutions, respectively. A simple visual check of the detector monitor that there was not any solid present would be confirmed by the absence of dark arching lines, which would have indicated a solid material scattering the X-rays. The MPS experiment for running a reaction which produced HKUST-1 was as follows:

Step 1: 600 μL of the copper salt solution was injected for 900 ms.
Step 2: 600 μL of the the ligand solution was injected for 1000 ms.
Step 3: 240 μL of the copper salt solution + 160 μL of the ligand solution were simultaneously injected for 100 ms.
Step 4: 5 μL of the ligand solution was injected for 3 ms.

The first two steps pushed out the solvent from the pipe lines inside of the stop-flow instrument, which were left there from the background measurement. The third step injected the amount of reagents from the system for the 6:4 copper salt to ligand reaction. The final step was a “cleaning step”, removing any solid which might have been left in the micromixer.

It was convenient for us to simultaneously control the shutter, detector, and stop-flow instrument using a “master control” program called the HCI (Histogram Control Interface). In this configuration the shutter would be opened manually, whereupon the HCI would “trigger” the stop-flow instrument to begin the experiment and simultaneously direct the detector to begin collecting measurements. This was advantageous so that the timing of the detector to collect measurements would be synchronized with the timing of the stop-flow instrument. This configuration eliminated the need to manually activate the stop-flow with the MPS program, and

instead only required one of us to start the detector, which would then wait for the signal from the HCI before collecting measurements.

4. Results

During two different beamtimes, the first from February 21, 2015 to February 16, 2015, and the second from July 13, 2015 to July 14, 2015, we have studied the formation of HKUST-1 by time-resolved SAXS. Our beamtime during February allowed us to become more familiar with and to optimize our use of the instrument, which would prove to be beneficial during the second beamtime. Our four days of beamtime in February allowed us to run nearly 50 reactions, which focused on reactions with $Cu(NO_3)_2 \cdot 2.5H_2O$ and $Cu(OAc)_2 \cdot H_2O$. During the July beamtime, our experiments focused on the less explored reactions using the reagents $CuCl_2 \cdot 2H_2O$ and $CuSO_4$.

Prior to running HKUST-1 reactions for both beamtimes, we ran a series of experiments in order to calibrate the stop-flow instrument and detector. In order to test the effectiveness of the stop-flow instrument, samples of a concentrated solution containing the bovine serum albumin (BSA) protein were prepared in an aqueous solution and loaded into one port in the stop-flow instrument. The BSA protein has a clearly defined SAXS pattern, making it useful for this analysis [12]. Deionized water was loaded into a different port from the BSA in the stop-flow instrument, and four experiments were conducted by injecting an amount of the protein with an amount of water which diluted the protein. Specifically the ratios of BSA to water which were measured were 1:9, 1:4, 2:3, and 1:0, for the four experiments respectively. The change in concentration of the protein in water affects the intensity of the X-ray scattering intensity. For a range of BSA concentrations, the trend we expected to see for increased X-ray scattering intensity with increased BSA concentration was confirmed [12].

4.1 Experiments from February 2015

The experiments we carried out during our four-day beamtime in February of 2015 were focused on analyzing reactions which we had known to form HKUST-1 nearly instantaneously. Table 1 shows a list of the first experiments conducted during this beamtime, which provided us with a consistent procedure for running stop-flow experiments. While these experiments did not provide any direct information about the formation of HKUST-1, this initial list of experiments built the foundation for our later successful experiments.

As can be seen from Table 1, all of these reactions were between aqueous $Cu(OAc)_2 \cdot H_2O$ and a solution of H_3TMA in methanol. Reactions involving $Cu(OAc)_2 \cdot H_2O$ were among the fastest reactions we found from our experiments in 2014, and so were a good candidate to begin our beamtime with. Primarily, the difficulties we faced for experiments A through U were attributable to the mechanics of the first set-up we used, which was different from the set-up in Figure 1. This alternative set-up, which is shown in Figure 3, was used in order to accommodate a second detector so that we could simultaneously collect SAXS and wide-angle X-ray scattering (WAXS) measurements.

During our preliminary experiments in 2014, we had used a configuration which allowed us to simultaneously measure SAXS and WAXS measurements. While SAXS allowed us to collect data which provided structural information on the initial amorphous solids and crystalline product, WAXS provided information about the larger crystalline lattice that is formed for HKUST-1. The graphs which resulted from WAXS data analysis are identical to the classic diffractograms seen from powder XRD studies. While our studies would have been improved by including WAXS studies, the SAXS studies provided the more critical information we sought.

Table 1. Each experiment corresponds to a reaction from February 2015 where HKUST-1 was synthesized by the reaction between a copper salt prepared in a solution of the indicated solvent, and a solution of the ligand (H_3TMA) prepared in the indicated solvent. The exposure time is the frequency by which a measurement was taken for S/WAXS, and there were 1000 measurements (frames/images) collected for each experiment.

Experiment	**Copper Salt**	**Copper Salt Solvent**	**Ligand Solvent**	**Exposure Time (s)**
A	$Cu(OAc)_2 \cdot H_2O$	Water	Methanol	1.000
B	$Cu(OAc)_2 \cdot H_2O$	Water	Methanol	1.000
C	$Cu(OAc)_2 \cdot H_2O$	Water	Methanol	1.000
D	$Cu(OAc)_2 \cdot H_2O$	Water	Methanol	0.250
E	$Cu(OAc)_2 \cdot H_2O$	Water	Methanol	1.000
F	$Cu(OAc)_2 \cdot H_2O$	Water	Methanol	1.000
G	$Cu(OAc)_2 \cdot H_2O$	Water	Methanol	1.000
H	$Cu(OAc)_2 \cdot H_2O$	Water	Methanol	1.000
I	$Cu(OAc)_2 \cdot H_2O$	Water	Methanol	1.000
J	$Cu(OAc)_2 \cdot H_2O$	Water	Methanol	1.000
K	$Cu(OAc)_2 \cdot H_2O$	Water	Methanol	0.250
L	$Cu(OAc)_2 \cdot H_2O$	Water	Methanol	1.000
M	$Cu(OAc)_2 \cdot H_2O$	Water	Methanol	1.000
N	$Cu(OAc)_2 \cdot H_2O$	Water	Methanol	1.000
O	$Cu(OAc)_2 \cdot H_2O$	Water	Methanol	1.000
P	$Cu(OAc)_2 \cdot H_2O$	Water	Methanol	1.000
Q	$Cu(OAc)_2 \cdot H_2O$	Water	Methanol	1.000
R	$Cu(OAc)_2 \cdot H_2O$	Water	Methanol	0.250
S	$Cu(OAc)_2 \cdot H_2O$	Water	Methanol	1.000
T	$Cu(OAc)_2 \cdot H_2O$	Water	Methanol	1.000
U	$Cu(OAc)_2 \cdot H_2O$	Water	Methanol	1.000

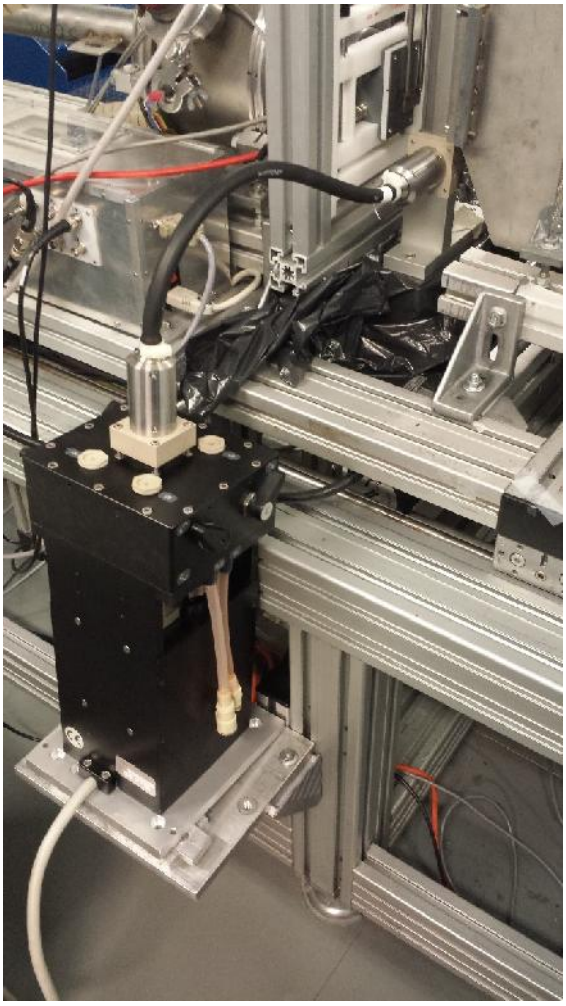

Figure 3. Alternative configuration of the stop-flow set-up from Figure 1, permitting S/WAXS measurements.

The long black tube seen in Figure 3 connecting the stop-flow instrument to the cuvet contains small plastic tubes, extending the distance the samples traveled. This tube caused several major problems during the first two and a half days of our beamtime, preventing quality data collections. It wasn't until late during the third day that we changed the stop-flow set-up to the configuration seen in Figure 1 and sacrificed our ability to collect WAXS measurements. Additional problems which arose were the blockage of the micromixer, which caused highly turbulent mixing, and incorrect mechanical settings on the stop-flow instrument.

There was also a lot of troubleshooting throughout the experiments in order to determine the optimal MPS settings, since in some cases the reagents would not be injected far enough to reach the micromixer or capillary. In order to prevent continual blockages of the micromixer and to prevent leaving residual samples in the capillary, thereby affecting the results of the next experiment, we would thoroughly clean the instrument following each experiment. It was not until experiment V that we had changed to the SAXS-only stop-flow set-up and managed to develop a consistent and reproducible experimental protocol. Table 2 shows the list of experiments where we had applied our experimental methodology to gain a number of successful experiments.

Table 2. List of successful experiments from the February 2015 beamtime. Experiments which are marked red did not produce quality results. Note that these experiments only collected SAXS measurements.

Experiment	**Copper Salt**	**Copper Salt Solvent**	**Ligand Solvent**	**Exposure Time (s)**
V	$Cu(OAc)_2 \cdot H_2O$	Water	Methanol	1.000
W	$Cu(OAc)_2 \cdot H_2O$	Water	Methanol	0.250
X	$Cu(OAc)_2 \cdot H_2O$	Water	Ethanol	1.000
Y	$Cu(OAc)_2 \cdot H_2O$	Water	Ethanol	2.000
Z	$Cu(OAc)_2 \cdot H_2O$	Water	Isopropanol	1.000
Aa	$Cu(OAc)_2 \cdot H_2O$	Water	Ethanol	0.250
Ab	$Cu(OAc)_2 \cdot H_2O$	Water	Ethanol	0.250
Ac	$Cu(OAc)_2 \cdot H_2O$	Water	Ethanol	1.000
Ad	$Cu(OAc)_2 \cdot H_2O$	Water	Isopropanol	0.250
Ae	$Cu(NO_3)_2 \cdot 2.5H_2O$	Water	Methanol	2.000
Af	$Cu(NO_3)_2 \cdot 2.5H_2O$	Water	Methanol	4.000
Ag	$Cu(NO_3)_2 \cdot 2.5H_2O$	Methanol	Methanol	1.000
Ah	$Cu(NO_3)_2 \cdot 2.5H_2O$	Ethanol	Ethanol	1.000
Ai	$Cu(NO_3)_2 \cdot 2.5H_2O$	Ethanol	Ethanol	0.250
Aj	$Cu(NO_3)_2 \cdot 2.5H_2O$	Water	Ethanol	1.000
Ak	$Cu(NO_3)_2 \cdot 2.5H_2O$	Water	Ethanol	0.250
Al	$Cu(NO_3)_2 \cdot 2.5H_2O$	Water	Isopropanol	1.000
Am	$Cu(NO_3)_2 \cdot 2.5H_2O$	Water	Isopropanol	1.000
An	$Cu(NO_3)_2 \cdot 2.5H_2O$	Water	Isopropanol	0.250
Ao	$Cu(NO_3)_2 \cdot 2.5H_2O$	Isopropanol	Isopropanol	1.000

Reactions which used isopropanol were largely unsuccessful since this alcohol produced a high pressure within the stop-flow instrument, making the alcohol difficult to load into the instrument. Experiments Aa and Aj did not produce any useful results towards the mechanism of formation of HKUST-1 after extensive data analysis, so they were also designated as poor experiments. One of the major advantages of using the stop-flow instrument was the ability to achieve extremely short time resolution experiments, in other words to take a measurement very quickly. In this beamtime, we took measurements as fast as every 250 milliseconds (ms, 0.250 s).

After an experiment had been completed, the data would be partially analyzed immediately to determine if we needed to re-run the reaction with a faster time resolution. Each reaction would initially be conducted at 1.000 s and then would be shorted to 250 ms (0.250 s) if a second experiment was required. In some cases we used a slower time resolution if the reagents had injected, but had yet to react. This was only done for reactions Y, Ae, and Af which had time resolutions of 2.000 s, 2.000 s, and 4.000 s, respectively.

4.2 Experiments from July 2015

Using our improved experimental procedures developed during the February 2015 beamtime, we turned our focus to examining reactions using the sparsely studied $CuCl_2 \cdot 2H_2O$ and $CuSO_4$ reagents. We also repeated some experiments from the February 2015 beamtime in order to verify the reproducibility of these experiments. Table 3 provides a complete list of our experiments for this second beamtime allocation.

Table 3. Experiments performed in July 2015 studying the formation of HKUST-1 by time-resolved SAXS. Experiments marked in red indicate a reaction with bad results.

Experiment	Copper Salt	Copper Salt Solvent	Ligand Solvent	Exposure Time (s)	Number of Frames
A	$CuCl_2 \cdot 2H_2O$	Water	Water	1.000	1000
B	$CuCl_2 \cdot 2H_2O$	Methanol	Water	1.000	1000
C	$CuCl_2 \cdot 2H_2O$	Methanol	Water	1.000	1000
D	$CuCl_2 \cdot 2H_2O$	Methanol	Water	0.500	500
E	$CuCl_2 \cdot 2H_2O$	Methanol	Water	0.500	500
F	$CuCl_2 \cdot 2H_2O$	Methanol	Water	0.500	500
G	$CuCl_2 \cdot 2H_2O$	Methanol	Water	0.100	500
H	$CuCl_2 \cdot 2H_2O$	Ethanol	Water	0.500	500
I	$CuCl_2 \cdot 2H_2O$	Ethanol	Water	0.100	500
J	$CuCl_2 \cdot 2H_2O$	Water	Methanol	0.100	500
K	$CuCl_2 \cdot 2H_2O$	Water	Methanol	1.000	1000
L	$CuCl_2 \cdot 2H_2O$	Water	Ethanol	1.000	1000
M	$CuCl_2 \cdot 2H_2O$	Water	Ethanol	1.000	500
N	$CuSO_4$	Water	Ethanol	1.000	500
O	$CuSO_4$	Water	Ethanol	0.500	500
P	$CuSO_4$	Water	Ethanol	0.100	500
Q	$Cu(NO_3)_2 \cdot 2.5H_2O$	Methanol	Water	0.100	1000
R	$Cu(NO_3)_2 \cdot 2.5H_2O$	Ethanol	Water	0.100	1000
S	$Cu(NO_3)_2 \cdot 2.5H_2O$	Ethanol	Ethanol	0.100	1000
T	$Cu(NO_3)_2 \cdot 2.5H_2O$	Methanol	Methanol	0.100	1000
U	$Cu(OAc)_2 \cdot H_2O$	Water	Methanol	0.100	1000
V	$Cu(OAc)_2 \cdot H_2O$	Water	Methanol	0.100	1000
W	$Cu(OAc)_2 \cdot H_2O$	Water	Ethanol	1.000	1000
X	$Cu(OAc)_2 \cdot H_2O$	Water	Ethanol	1.000	1000

Only three reactions during this beamtime resulted in experimental errors, which was significantly less compared with the over 30 experiments from the February 2015 beamtime. This contrast shows the effectiveness of the procedural methodology we had developed for these stop-flow in-situ MOF synthesis experiments during the February beamtime. In the cases of D and F, the settings on the stop-flow instrument were not set appropriately, so the reagents did not

inject and no reaction was observed. Reaction L provided poor data because the syringe at the end of the capillary had loosened, and the reagents were leaking out. Each of these reactions was repeated affording us a successful reaction and quality data set. The improved experimental protocol also permitted us to quickly run reactions which we determined after the beamtime to still have an insufficient time resolution. During the July beamtime, we also ran reactions with time resolutions as fast as 100 ms. Our strategy for this beamtime was to establish trends for reaction and nucleation kinetics and changes in crystal structure as a function of the solvent. Furthermore, we can now compare different reactions for these same parameters for all four copper salts with common solvents across the two beamtimes.

4.3 Data Analysis

The experimental work of taking measurements on the beamline lasted for only a total of six days, however for each of those days we conducted experiments for an average of 15 hours. Still, arguably the lengthiest and most difficult part of this work was the data analysis. In single-crystal XRD, another crystal structure characterization technique with similarities to SAXS, there are a variety of readily available software packages, like APEX II which allows for quick data analysis [13]. I am not aware of any such data analysis software packages for SAXS and more commonly (as is the case at the Austro-SAXS beamline) unique programs are written by the beamline scientists themselves and annexed into a computational graphics software package.

At the Austro-SAXS beamline, the program used to process the data collected by the detector is called FIT2D [14]. For a scattered X-ray from the sample, the detector measures the intensity of the scattered X-ray, and then measures two angles (θ and φ) which provide the position and orientation of the scattered X-ray with respect to the incident X-ray beam. These raw data sets are two-dimensional, where the intensity is considered as a function of θ and φ. The

program FIT2D simplifies this to a one dimensional data set, where the intensity considered only as a function of a value called the scattering vector (q). The definition of the scattering vector is:

$$q = \frac{4\pi}{\lambda} \sin \varphi$$

where λ is the wavelength of the X-ray [15].

The scattering vector provided a convenient way to plot our results on a Cartesian graph. The program IGOR Pro 6 was used to perform in-depth data analysis of the one-dimensional data sets and to graphically display the results [16]. Figure 4 provides an example of a graph from one of our experiments which plots the intensity, I, of the data set as a function of the scattering vector, q.

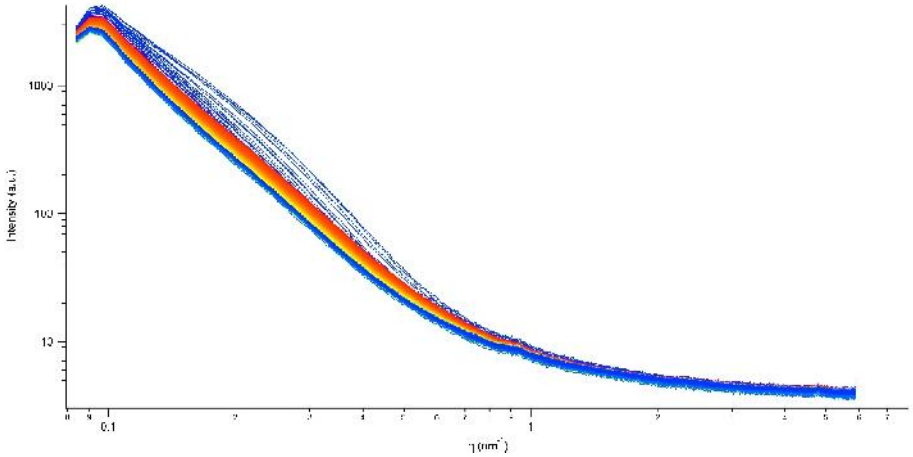

Figure 4. The I vs. q graph for experiment U from the July 2015 beamtime. Note that q has units of inverse nanometers (nm^{-1}) and intensity has arbitrary units (a. u.).

The graph in Figure 4 is depicted in a logarithmic scale in order to provide a clearer image. Each line in an I vs. q plot indicates one measurement taken from the detector. Based on certain shape characteristics of these I vs. q graphs, we can deduce structural features about the sample. As an example for the I vs. q graph for experiment U seen in Figure 4, a “bump” feature composed of the slightly dispersed blue lines can be seen in the first one third of the graph. This type of feature is typical of nanoparticle formation in SAXS data analysis.

The next step for analyzing the data is to normalize the data, which provides a level of homogeneity across all of the data sets. When the data is normalized, transmission effects and the primary intensity (intensity of the beam from the storage ring of the synchrotron) are set to be the same for all data sets. The result is an I vs. q plot, like the one shown in Figure 5, where the data set appears more uniform.

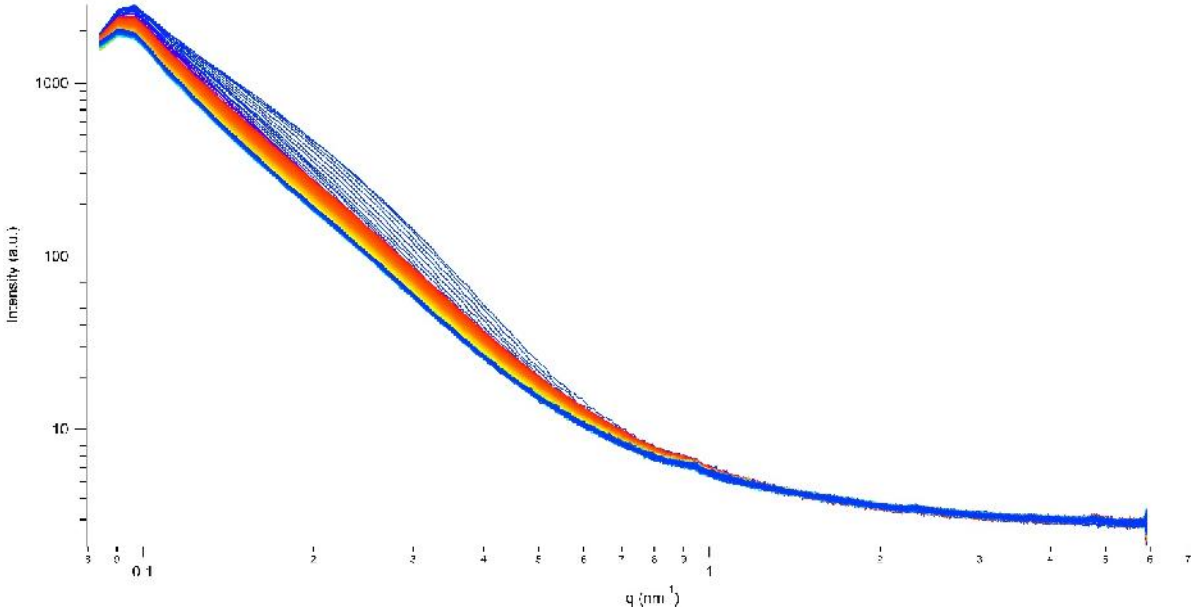

Figure 5. Normalized I vs. q plot for experiment U from the July 2015 beamtime. Note the more regular spacing of the "bump" feature as compared to the plot in Figure 4.

From a normalized I vs. q plot we can perform several different forms of data analysis, including evaluating the intensity and position of the first-order Bragg peak (if there is one). The first-order Bragg peak is a distinct peak seen protruding vertically from the I vs. q plot. These peaks are an indication of the formation of a crystalline solid, and are unique to a particular crystal plane. Figure 6 shows a zoomed image of the peak in Figure 5.

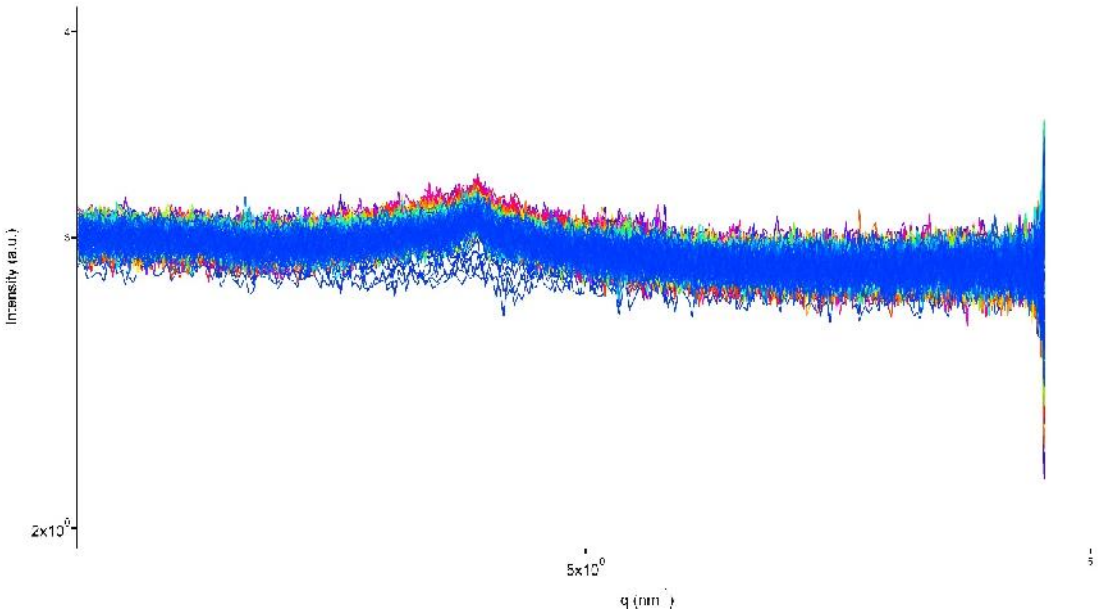

Figure 6. The first-order Bragg peak from reaction U. The peak is located at q = 4.8 nm^{-1}.

Ideally these peaks will appear sharp and well defined, without significant background or noise. The scattering vector value for the first-order Bragg peak can be related to a d-space value, something that is more common and familiar from conventional X-ray diffraction studies. The calculation of the d-space value is simply [15]:

$$d = \frac{2\pi}{q}$$

Since we have taken time-resolved measurements during these beamtimes, we can also analyze the development of the first-order Bragg peak. Figure 7 provides one example of this type of analysis.

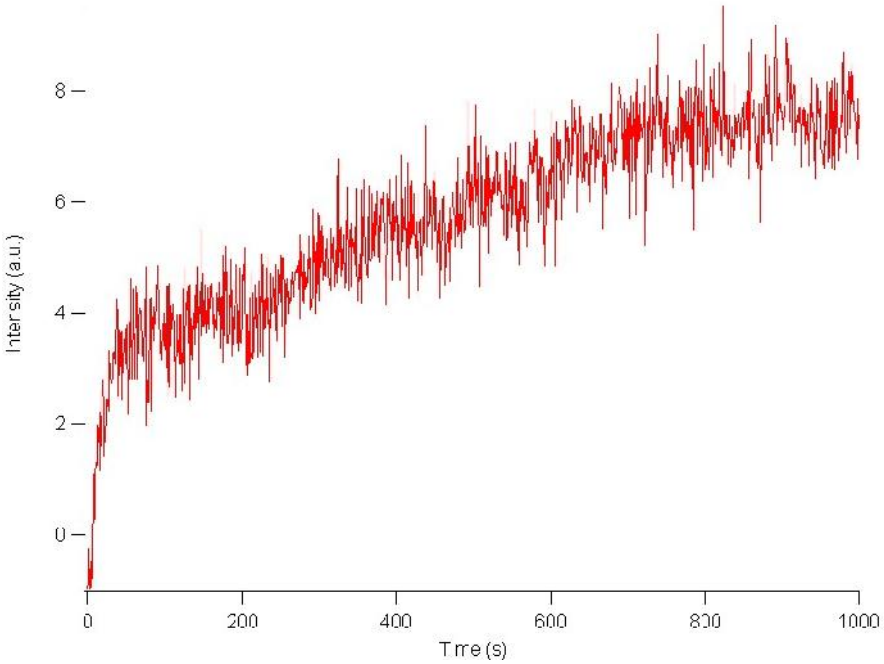

Figure 7. Development of the first-order Bragg peak as a function of time for experiment V from the February 2015 beamtime. Immediate rapid growth is seen, which after about 50 s slows down to a slower growth rate which remains approximately constant for the remainder of the reaction.

Other important information which can be discerned from the normalized I vs. q plot would be the integrated intensity and the Porod invariant. More significantly, these two values are used to calculate the correlation length, a measure of the growth of the amorphous solid material in the sample. A plot of all three values as a function of time is shown in Figure 8. Here, we see an immediate and rapid growth of solid material, which then is seen to rapidly dissipate, and then finally grow steadily beginning at approximately 100 s.

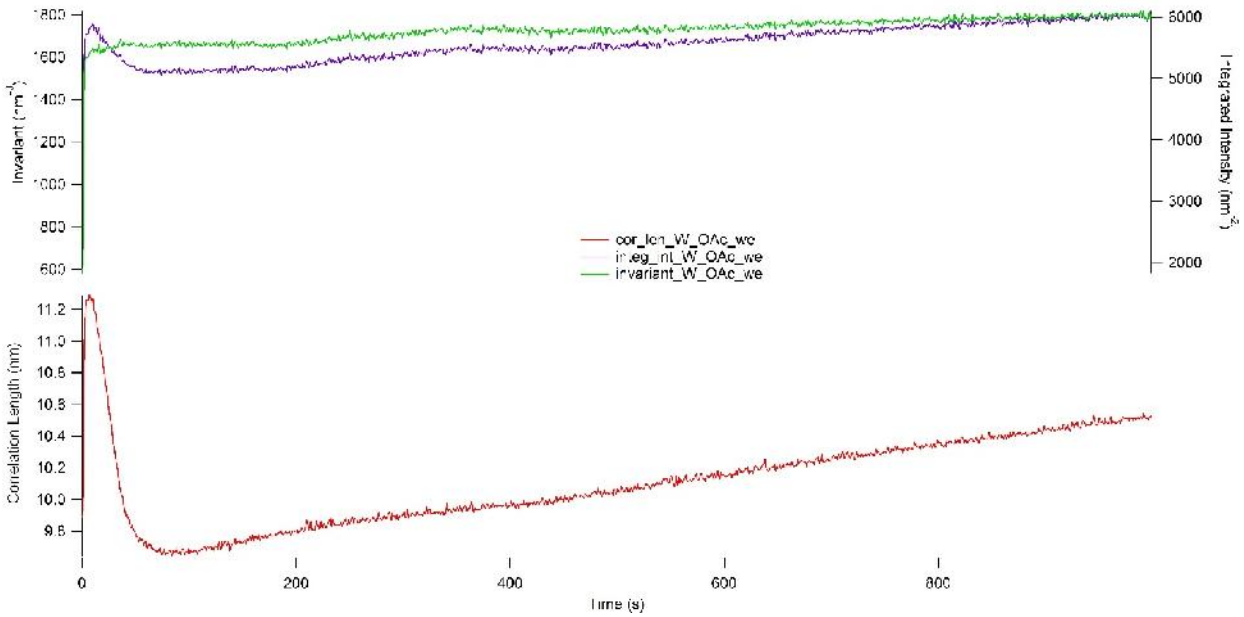

Figure 8. Plot of the correlation length, integrated intensity, and invariant as a function of time for experiment W from the July 2015 beamtime.

One final manipulation of the I vs. q plots must be performed before a final determination should be made regarding the quality of that particular data set. This final step is to carefully subtract the background. Prior to each experiment, a small number of background frames are measured to ensure there is no residue in the capillary from a previous experiment, but also to get the scattering profile of the solvent or any other "non-sample" materials which might have contributed to the scattering curve. An example of a background subtracted and normalized I vs q plot is shown in Figure 9. Ideally these types of I vs. q plots should adopt a "spoon" shape, and the top of the "circular" part of the spoon should be close to parallel with the x-axis.

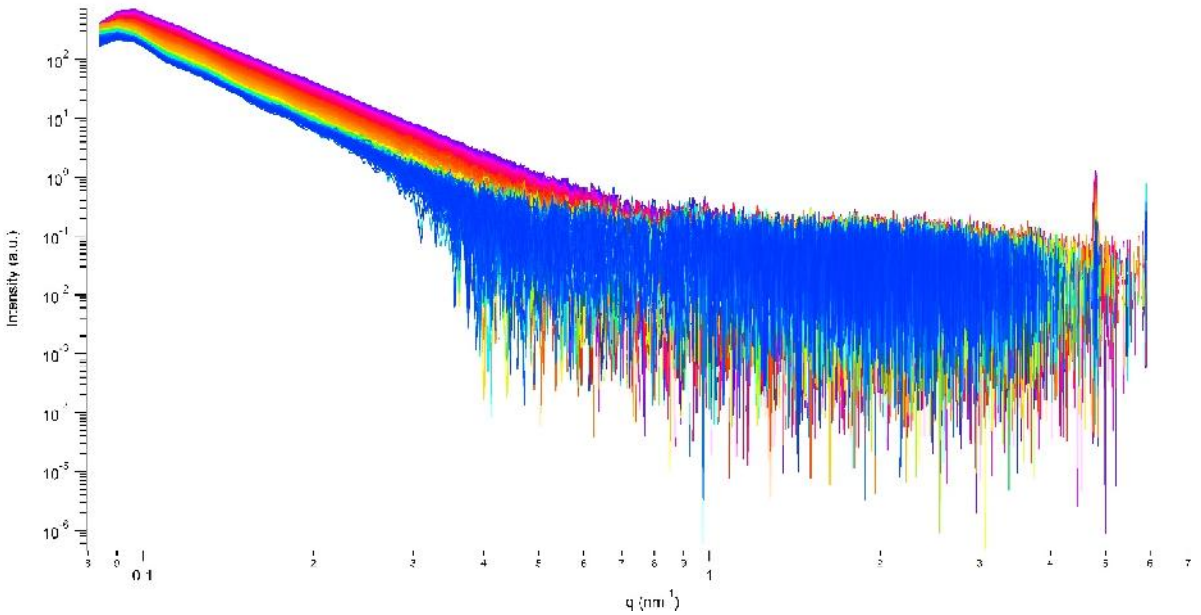

Figure 9. Background subtracted and normalized I vs. q plot for experiment C from the July 2015 beamtime.

Conclusion

More complex data analysis which requires a high level of experience and knowledge with computer programming and curve fitting is ongoing. This will require several more months before being completed, since the most recent beamtime was in July and on average data anlysis takes approximately six months to complete. Based on the data analysis already completed, we have begun to extract trends which clearly demonstrate that the solvent and anion of the copper salt profoundly affect the rate that HKUST-1 is formed, the identity of the final crystalline product, and information about the mechanism by which HKUST-1 forms.

This work constitutes the first example we have been able to find where a stop-flow instrument has been used to not only synthesize MOFs, but also to be used in conjunction with X-ray scattering studies. We are excited about the potential for this instrument to be used for in-situ studies of other MOF systems. Our SAXS studies achieved time resolutions as fast as 100 ms, providing structural data in the most critical parts of the formation of HKUST-1. In these early parts of the reactions, the data we have gained describes the growth of the material, in

addition to elucidating the pathway for which these materials form. Furthermore, this study has proven the effectiveness of time-resolved SAXS as a structural characterization method in order to gain critical information for the mechanism of the formation of MOFs.

Acknowledgements

My biggest thanks goes to Dr. Heinz Amenitsch, the managing beamline scientist for the Austro-SAXS beamline and a professor at the Graz University of Technology. Dr. Amenitsch was incredibly supportive of me and has been a great and fun mentor. Next I must recognize my advisor at Syracuse University, Dr. Karin Ruhlandt, who has enthusiastically supported my ambitions for participating in international collaborative research, and for funding my participation in the NESY European Winterschool & Symposium on Synchrotron Radiation in Altausee, Austria. I want to thank my other collaborators who I have worked with through TU Graz, especially Dr. Ana Torvisco, crystallographer at TU Graz, and Dr. Manfred Kriechbaum, SAXS scientist at TU Graz. I want to also thank everyone who I worked with at the Austro-SAXS beamline: Sigrd Bernstorff, Barbara Sartori, Benedetta Marmiroli, Marco de Marco, Krunoslav Juraič, and Max Burian for treating me like family and being great co-workers and friends.

I would like to thank the Marshall Plan Foundation for facilitating this collaboration between TU Graz and Syracuse University through the generous fellowship made available to me. I would also like to recognize the Max Kade Foundation for providing travel grants to me, I would not have been able to participate in this collaboration without their support. I would like to express a huge thanks to Katrin Landfahrer, the Marshall Plan Fellowship coordinator at TU Graz, who was always available and ready to help me navigate any problems I faced while I was in Graz. I would like to thank Dr. Frank Uhlig, the Dean of the Institute of Inorganic Chemistry

at TU Graz, for his continued support over my work with TU Graz extending over the last two years. I want to thank all of the friends I've made at TU Graz and at the Elettra Synchrotron for their support, especially everyone at the Institute of Inorganic Chemistry.

References

[1] Kitagawa, S.; Kitaura, R.; Noro, S.-I. *Angew. Chem. Int. Ed.*, **2004**, *43*, 2334-2375.
[2] Chang, Z.; Yang, D.-H.; Xu, J.; Hu, T.-L.; Bu, X.-H. *Adv. Mater.*, **2015**, *27*, 5432-5441.
[3] Yaghi, O. M.; O'Keeffe, M.; Ockwig, N.; Chae, H.; Eddaoudi, M.; Kim, J. *Nature*, **2003**, *423* (6941), 705-714.
[4] Stock, N.; Biswas, S. *Chem. Rev.*, **2012**, *112*, 933-969.
[5] Chui, S. S.-Y.; Lo, S. M.-F.; Charmant, J. P. H.; Orpen, A. G.; Williams, I. D. *Science*, **1999**, *283*, 1148-1150.
[6] Roy, A.; Srivastava, A. K.; Singh, B.; Shah, D.; Mahato, T. H.; Srivastava, A. *Dalton Trans.*, **2012**, *41* (40), 12346-12348.
[7] Peng, Y.; Krungleviciute, V.; Eryazici, I.; Hupp, J. T.; Farha, O. K.; Yildirim, T. J. *J. Am. Chem. Soc.*, **2013**, *135*, 11887-11894.
[8] Xiao, B.; Wheatley, P. S.; Zhao, X.; Fletcher, A. J.; Fox, S.; Rossi, A. G.; Megson, I. L.; Bordiga, S.; Regli, L.; Thomas, K. M.; Morris, R. E. *J. Am. Chem. Soc.*, **2007**, *129*, 1203-1209.
[9] Huo, J.; Brightwell, M.; El Hankari, S.; Garai, A.; Bradshaw, D. *J. Mater. Chem. A*, **2013**, *1*, 15220-15223.
[10] Loera-Serna, S.; Núñez, L. L.; Flores, J.; López-Simeon, R.; Beltrán, H. I. *RSC Adv.*, **2013**, *3*, 10962-10972.
[11] Bajpe, S. R.; Kirschhock, C. E. A.; Aerts, A.; Breynaert, E.; Absillis, G.; Parac-Vogt, T. N.; Giebeler, L.; Martens, J. A. *Chem. Eur. J.*, **2010**, *16*, 3926-3932.
[12] Zhang, F.; Skoda, M. W. A.; Jacobs, R. M. J.; Martin, R. A.; Martin, C. M.; Schreiber, F. *J. Phys. Chem. B*, **2007**, *111*, 251-259.
[13] APEX II: Bruker AXS Inc.
[14] FIT2D: Hammersley, A. P., European Synchrotron Radiation Facility (ESRF), Grenoble, France.
[15] Schnablegger, H.; Singh, V. "The SAXS Guide", 3rd Ed., Anton Paar: Graz, Austria.
[16] IGOR Pro 6: Wavemetrics Inc., Lake Oswego, Oregon.